Synthesis and phase behaviour of a homologous series of polymethacrylate-based side-chain liquid crystal polymers

Article

Accepted Version

Cook, A. G., Inkster, R. T., Martinez-Felipe, A., Ribes-Greus, A., Hamley, I. ORCID: https://orcid.org/0000-0002-4549-0926 and Imrie, C. T. (2012) Synthesis and phase behaviour of a homologous series of polymethacrylate-based side-chain liquid crystal polymers. European Polymer Journal, 48 (4). pp. 821-829. ISSN 0014-3057 doi: 10.1016/j.eurpolymj.2012.01.021 Available at https://centaur.reading.ac.uk/27783/

www.reading.ac.uk/centaur

CentAUR

Central Archive at the University of Reading

Reading's research outputs online

Synthesis and phase behaviour of a homologous series of polymethacrylate-based side-chain liquid crystal polymers

Andrew G. Cook[a], Rachel T. Inkster[a], Alfonso Martinez-Felipe[b], Amparo Ribes-Greus[b], Ian W. Hamley[c] and Corrie T. Imrie[a]*

[a] Chemistry, School of Natural and Computing Sciences,
University of Aberdeen, Aberdeen AB24 3UE, Scotland, UK

[b] Institute of Materials Technology, Universitat Politècnica de València,
Camino de Vera S/N, 46022 Valencia, Spain

[c] Department of Chemistry, University of Reading, Whiteknights, Reading
RG6 6AD, UK

* Corresponding author. Email c.t.imrie@abdn.ac.uk

Abstract

The homologous series of side chain liquid crystal polymers, the poly[ω-(4-methoxyazobenzene-4'-oxy)alkyl methacrylate]s, has been prepared in which the length of the flexible alkyl spacer has been varied from 3 to 11 methylene units. All the polymers exhibit liquid crystalline behaviour. The propyl and butyl members show exclusively nematic behaviour. The pentyl, hexyl, octyl and decyl members show a nematic and a smectic A phase while the heptyl, nonyl and undecyl homologues exhibit only a smectic A phase. The smectic A phase has been studied using X-ray diffraction and assigned as a smectic A_1 phase in which the side chains are fully overlapped and the backbones are confined to lie between the smectic layers. For the nonyl member an incommensurate smectic phase is observed. The dependence of the transition temperatures on the length of the flexible spacer is understood in terms of the average shapes of the side chains.

1.   Introduction

Side chain liquid crystal polymers continue to be the focus of considerable research activity over thirty years after their initial discovery [1]. This interest arises not only as a result of their considerable application potential in a wide range of electro-optic technologies but also because they provide a demanding challenge to our fundamental understanding of the molecular factors that promote self-assembly in condensed systems. A side chain liquid crystal polymer contains three structural components: a liquid crystal or mesogenic group, a polymer backbone and connecting these, a flexible alkyl spacer. In essence, the anisotropic interactions between the mesogenic groups give rise to the observation of liquid crystalline behaviour while the flexible spacer decouples the opposing tendencies of the liquid crystal groups to self-assemble from those of the polymer backbones to adopt random coil conformations. In consequence, these polymers exhibit a unique duality of properties and show the electro-optic characteristics of low molar mass liquid crystals, albeit on a much slower timescale, together with macromolecular properties such as glassy behaviour and mechanical integrity.

In recent years, liquid crystal polymer-based photosensitive films have attracted intense interest [2-4] These polymers often contain azobenzene-based mesogenic groups for which the reversible *trans-cis* photoisomerisation can be utilised to control the phase behaviour [5,6] and hence, optical properties (for recent examples, see, [7-13]) and photomechanical properties of the film (for recent examples, see, [14-19]). One of the more commonly used azobenzene-based mesogenic groups in the design of photochromic side chain liquid crystal polymers is 4-methoxyazobenzene (see, for example, [20-22]) and in particular, much interest has focussed on the properties of the poly[ω-(4-methoxyazobenzene-4'-oxy)alkyl methacrylate]s [23-40];

1
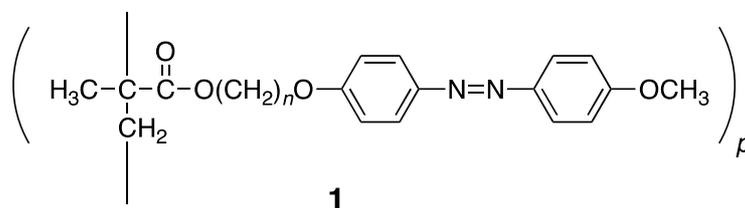
which are referred to here using the acronym *n*-MeOAzB in which *n* denotes the number of methylene units in the flexible alkyl spacer. Although 6-MeOAzB has been the most extensively studied member of this series [23-40], other homologues, $n = 2-6, 8, 10$ and 12, have also been reported. Surprisingly, however, just one report focuses on the liquid crystalline behaviour of the polymers ($n = 6, 8, 10, 12$) and

investigates phase structure [40] but such a study of the phase behaviour of the complete homologous series would allow for the rational design of new polymers having tailored phase behaviour. To correct this surprising omission from the literature, we report here for the first time the synthesis and liquid crystal properties of this important series of side chain liquid crystal polymers.

2.   Experimental

The *n*-MeOAzB series was prepared according to the synthetic route shown in Scheme 1. The syntheses of 4-methoxy-4'-hydroxyazobenzene, **2**, [41], the α-bromo-ω-(4-methoxyazobenzene-4'-oxy)alkanes, **3**, [42] and the ω-(4-methoxyazobenzene-4'-oxy)alkyl methacrylates [41] have been described in detail elsewhere. The polymerization method was identical in each case and a representative description is provided for 8-MeOAzB. Benzene was distilled over calcium hydride. AIBN was recrystallized from toluene, washed with petrolueum spririts (80-100˚C) and dried under vacuum. All other reagents were used as received from Sigma-Aldrich.

2.1   Polymerisation

The polymerization reaction was performed according to the method described by Craig and Imrie [43]. Thus, **4** (*n* = 8) (1 g) was dissolved in benzene (10 ml) and 1 mol% AIBN added as initiator. The reaction mixture was degassed under vacuum using the freeze-pump-thaw method, and flushed with argon for 20 min. The reaction mixture was heated in a water bath at 60 °C to initiate the polymerisation. After 48 h, the reaction mixture was precipitated into a large amount of methanol, the precipitate collected, redissolved in chloroform, and reprecipitated using methanol. The removal of monomer from the polymer was assessed spectroscopically by the disappearance of the alkene signals in the IR (1633 cm^{-1}) and ^{1}H NMR (5.5 and 6.1 ppm) spectra. 8-MeOAzB: Yield 68%. ^{1}H NMR (CDCl$_3$) δ: 7.8, 6.9 (m, 8 H, aromatic rings), 4.1-3.9 (m, 4 H, OCH$_2$), 3.8 (s, 3 H, OCH$_3$), 2.1-0.8 (m, 14 H, CH$_2$ spacer, CH$_2$ backbone, m, 3 H, CH$_3$). IR (KBr) ν cm^{-1}: 1726 (C=O).

2.2   Characterization

The structures of all the polymers and their intermediates were confirmed using ^{1}H-NMR and FTIR spectroscopy. ^{1}H-NMR spectra were measured in CDCl$_3$ on either a Varian Unity Inova 400 MHz or a Bruker AC-F 250 MHz spectrometer. FTIR spectra were recoded using an ATI Mattson spectrometer. The molecular weights of the polymers were measured by gel permeation chromatography (GPC) using a Knauer Instruments chromatograph equipped with two PL gel 10 μm mixed columns and controlled by Polymer Laboratories GPC SEC V5.1 Software. Chloroform was used as the eluent. A calibration curve was obtained using polystyrene standards.

The thermal behaviour of the polymers was investigated using a Mettler Toledo DSC822^e differential scanning calorimeter equipped with a TSO 801RO sample robot and calibrated using indium and zinc standards. Two samples were used for each polymer and the results averaged. The time-temperature profile for all samples was heat, cool and reheat at 10°C min^{-1} with a 3-minute isotherm between heating and cooling segments. All samples were heated from 25°C to approximately 10°C above their clearing temperatures. Thermal data were normally extracted from the second heating trace. Phase characterisation was performed using polarised light microscopy using an Olympus BH2 polarising light microscope equipped with a Linkam TMS 92 hot stage. Clear, characteristic optical textures from which phase assignments were possible were obtained by cooling the polymer at 0.1 ˚C min^{-1} from *ca* 10 ˚C above the clearing the temperature into the phase in question.

SAXS/WAXS experiments were performed on station 8.2 at the SRS, Daresbury Laboratory. The X-ray wavelength was λ = 1.54 Å. For SAXS, the sample-to-detector distance was 1.1 m. The q = $4\pi\sin\theta/\lambda$ (2θ = scattering angle) scale was calibrated using collagen (rat tail tendon). Intensities were recorded using a gas-filled multiwire quadrant detector. For WAXS, a curved INEL linear detector was used. The WAXS scale was calibrated using HDPE.

3.   Results and Discussion

3.1 GPC Analysis
Table 1 lists the molecular weights, number-average-degrees of polymerisation and the polydispersities of the *n*-MeOAzB series, **1**. The number average molecular

weights of the polymers range from 7 000 to 32 300 g mol^{-1} with corresponding average degrees of polymerisation in the range 15 – 79. With the exception of 11-MeOAzB, these high molecular weights ensure that the thermal behaviour of the polymers do not lie within the molecular weight-dependent regime [44]. The thermal behaviour of 11-MeOAzB may lie on the border between the molecular weight dependent and independent regimes, but its molecular weight is sufficiently high to ensure that its transition temperatures are not strongly dependent on molecular weight [45].

3.2 Thermal Behaviour

The transitional properties of the *n*-MeOAzB series, **1**, are listed in Table 2. These data have been extracted from the second heating cycles of the DSC time-temperature profiles and the traces are collected in Figure 1. Nematic phases were assigned on the basis of the observation of a characteristic nematic *schlieren* texture when viewed through the polarised light microscope and a representative texture is shown as Figure 2(a). Smectic A phases were identified by the observation of a focal conic fan texture in coexistence with homeotropically aligned domains and a representative texture is shown as Figure 2(b).

The DSC traces shown by 3-MeOAzB and 4-MeOAzB both contain a weak second-order transition assigned as a glass transition and a single endothermic peak. When the isotropic phase was cooled for both polymers, a nematic *schlieren* texture developed. This assignment is supported by the small entropy change associated with the transition and which is comparable to that seen for other types of side-chain liquid crystal polymers [46] as well as for low molar mass liquid crystals [47]. This view was confirmed using X-ray diffraction. Specifically, no peaks were observed in the small angle region for either polymer, see Figure 3(a), while only broad peaks were observed at wide angles, see Figure 3(b). For 3-MeOAzB at 100 ˚C, the peaks in the wide angle are centred at 4.6 Å and 1.7 Å. The 4.6 Å spacing arises from the side-side packing of the mesogenic units and / or of the polymer chains, while the 1.7 Å peak is most likely to be associated with local correlations of the aromatic units.

The DSC traces for 5-MeOAzB, 6-MeOAzB and 8-MeOAzB contain two endothermic peaks and in addition, a weak second order transition. The latter has been assigned as a glass transition. On cooling the isotropic phase of each polymer, a nematic *schlieren* texture developed and this assignment is supported by the small entropy change associated with the clearing transition. On further cooling, bâtonnets

developed and coalesced to give a well-defined focal conic fane texture. Other areas of the preparation showed homeotropic alignment. The observation of focal-conic fans implies a layered structure, while the homeotropic alignment indicates an orthogonal arrangement of the director with respect to the layer planes. In consequence, this lower temperature phase is assigned as a smectic A phase and the associated entropy change is consistent with this view [48]. As we will see this phase assignment has been confirmed using X-ray diffraction. The DSC trace for 10-MeOAzB consists of a weak second order transition assigned as a glass transition and a rather broad endothermic peak. On cooling the isotropic phase, a nematic *schlieren* texture developed followed on further cooling by the formation of smectic A focal conic fan texture, see Figure 2. Similar phase behaviour was reported for this polymer by Zhu *et al* [40]. In order to obtain an estimate of the entropy changes associated with these transitions, Figure 4 shows the clearing endotherm deconvoluted into two component peaks and the transition temperatures and associated enthalpies obtained are wholly consistent with the phase changes observed using polarised light microscopy. The larger value of $\Delta S_{SmAN}/R$ shown by 10-MeOAzB is consistent with the McMillan theory [49] which predicts that the strength of the smectic A-nematic transition, as reflected by the transitional entropy, increases as the nematic range decreases [50]. Conversely, the smallest value of $\Delta S_{SmAN}/R$ is seen for 6-MeOAzB which exhibits the largest nematic range.

The smectic A phase assignment for 8-MeOAzB and 10-MeOAzB was confirmed using X-ray diffraction. Figure 5(a) shows the small angle region of the X-ray pattern obtained for the smectic A phase of 10-MeOAzB and a weak reflection is observed at 15.1 Å, while two broad peaks are seen in the wide angle centred at 4.5 Å and 1.7 Å (Figure 5(b)). The positions of these peaks do not vary significantly with temperature. Essentially identical X-ray patterns were observed for the smectic A phase of 8-MeOAzB with the very weak small angle reflection located at 12.9 Å. No clear small angle reflection was observed for the smectic A phase shown by 5-MeOAzB and 6-MeOAzB under the same experimental conditions. We shall discuss the structure of the smectic A phase later.

The DSC traces for 7-MeOAzB, 9-MeOAzB and 11-MeOAzB each show a weak second-order transition, assigned as the glass a transition, and an endothermic peak. On cooling the isotropic phase of each of these polymers, bâtonnets developed, coalescing to give a well-defined focal conic fan texture in coexistence with regions of

homeotropic alignment. Thus, this is assigned as a smectic A phase and the magnitude of the associated entropy change supports this view [51,52]. Figure 6 shows the X-ray diffraction patterns obtained at 115 ˚C for the smectic A phase of 9-MeOAzB. Two orders of reflection centred at 26.1 and 14.1 Å are seen in the small angle region while two broad peaks are seen in the wide angle centred at 4.4 Å and 1.7 Å. At higher temperatures, only the reflection centred at 14.2 Å is observed in the small angle region, see Figure 7(a), while no change is seen in the wide angle pattern, see Figure 7(b). Essentially identical X-ray patterns to those shown in Figure 7 were also seen for the smectic A phases of 7-MeOAzB and 11-MeOAzB; the small angle reflection was seen at 12.6 and 15.9 Å, respectively. For each of these polymers, only one small angle reflection was observed over the whole temperature range of the smectic A phase.

3.3 Structure of the smectic A phase

If we now turn our attention to the structure of the smectic A phase and first consider the smectic A phase shown by 9-MeOAzB. Figure 8 shows the temperature dependence of the small angle X-ray diffraction as a function of the scattering vector, q for 9-MeOAzB. These data show that the 14.2 Å reflection cannot be considered as the second order reflection of the 26.1 Å reflection because we see quite different temperature dependences for the two peaks. At low and high temperatures in the smectic A range, only the 14.2 Å reflection is observed. It is difficult to envisage an orthogonal smectic arrangement with such a small periodicity and an associated d/L ratio of *ca* 0.54. In low molar mass systems, this would be indicative of an intercalated smectic A phase observed for oligomeric mesogens [53-55]. However, such a packing arrangement is not possible for 9-MeOAzB. Instead, we propose that these polymers show a smectic A_1 phase in which the side-chains are fully interleaved as shown schematically in Figure 9(a). Presumably the driving force for the formation of this arrangement is to maximise the packing efficiency of the side chains while the backbones are confined to lie between the smectic layers. The d/L ratio for this packing arrangement should be *ca* 1 rather than the observed value of 0.54. We propose, however, that the symmetry of this smectic A_1 phase is such that the electron density profile is quasi-symmetric about the mid-point of the layer and the backbone domain between the layers. This symmetry accounts for the absence of the first order reflection in the small angle region of the X-ray pattern. A similar structure was proposed by Zhu *et al* [40] but they also observed the first order reflection at high temperatures.

On cooling, the Sm A_1 phase for 9-MeOAzB, we see the emergence of the 26.1 Å reflection (Figure 8) and this is approximately equal to the length of the side chain. We assign this to the formation of an incommensurate smectic phase in which domains of Sm A_1 packing coexist with regions in which side chains are packed in a parallel fashion as shown schematically in Figure 9(b). In such an arrangement the layer spacing is smaller than would be predicted for the smectic A_1 phase and this is consistent with the assignment of the 14.2 Å reflection as the second order reflection associated with smectic A_1 packing. In the smectic A_1 phase the alkyl spacers and aromatic units are fully mixed and this is unfavourable both energetically and entropically [56], providing the driving force for the formation of the domains in which the side chains are aligned in a parallel fashion. It is not clear, however, why on further cooling the 26.1 Å disappears and only the 14.2 Å reflection is observed. There is no evidence from either DSC or microscopy to suggest, however, that the appearance and disappearance of the 26.1 Å reflection is associated with phase transitions.

The arrangement of the side-chains in the smectic A phases shown by 7-MeOAzB, 8-MeOAzB, 10-MeOAzB and 11-MeOAzB is presumably the same as that shown in Figure 9(a) for 9-MeOAzB and for these polymers only the second order reflection associated with the smectic A_1 phase is seen in the small angle region of the X-ray diffraction patterns. This accounts for why these reflections are so weak and indeed are not observed for the smectic A phases seen for 5-MeOAzB and 6-MeOAzB. The *d/L* ratio for 7-MeOAzB is 0.53, 8-MeOAzB 0.52, 10-MeOAzB 0.53 and 11-MeOAzB 0.54. Smectic behaviour is not observed for 3-MeOAzB and 4-MeOAzB presumably because in these polymers the spacers are too short to accommodate the mesogenic groups in the SmA_1 arrangement shown in Figure 9(a).

3.4 Transitional Properties
The dependence of the transition temperatures on the length of flexible alkyl spacer, *n*, for the *n*-MeOAzB series is shown in Figure 10, and this includes data extracted from the literature for 2-MeOAzB [33] and 12-MeOAzB [40]. 2-MeOAzB is reported to exhibit only nematic behaviour [32] although a previous report described it as an amorphous polymer [27], while 12-MeoAzB exhibits a smectic A phase and a very narrow temperature range nematic phase [40]. The glass transition temperature, T_g, shows a significant decrease on passing from 2-MeOAzB to 3-MeOAzB. On further increasing *n*, a weak odd-even effect is seen in T_g in which polymers having odd values of *n* show the higher values. This odd-even effect is attenuated for the higher

values of n. The odd-even effect in T_g mirrors that seen for the SmA-N / I transition temperatures and we will return to this observation later. The glass transition temperatures for a homologous series of polymethacrylate-based side chain liquid crystal polymers typically decrease on increasing spacer length before reaching a limiting a value [43,45,48,57]. This behaviour is attributed to the plasticization of the backbone by the side chains [58]. For the n-MeOAzB series, this plasticization effect may be offset by the formation of the smectic A_1 phase which acts to confine the backbone to lie between the layers and hence reduces its mobility.

The clearing temperature also shows a significant decrease on passing from 2-MeOAzB to 3-MeOAzB. This is followed by an increase in the clearing temperature on moving to 4-MeOAzB before a small odd-even effect emerges in which polymers having odd values of n show the higher clearing temperatures. A considerably more pronounced alternation is seen in the SmA-N / I transition temperatures as n is increased. This odd-even effect is most often attributed to the alternation in the average shape of the side-chain and its effect on the relative orientation of the mesogenic groups on varying the parity of the spacer. Thus, for a spacer containing an even number of methylene units in the all-*trans* conformation, the mesogenic group is constrained to lie at some angle with respect to the polymer backbone whereas for an odd-membered spacer the mesogenic unit is orthogonal with respect to the backbone, see Figure 11. It is highly unlikely, however, that the spacer exists in a single conformation but there is a number of conformations containing a single *gauche* defect which preserve this orthogonal arrangement for odd membered spacers while no such conformations exist for an even membered spacer. The odd membered spacers can therefore pack more efficiently in the smectic A_1 phase resulting in higher transition temperatures. This rationalisation does assume that the backbone lies in a plane orthogonal to the director, and this view is supported by neutron scattering studies on a closely related polymethacrylate-based side chain liquid crystal polymer [58]. The attenuation of the alternation on increasing n may be explained by the dilution of this shape change resulting from the greater number of conformations available to the spacer as its length is increased. The alternation in the glass transition temperatures seen for intermediate values of n can also be explained within this framework and specifically, the odd-membered spacers allow for more effective packing of the side chains and hence a decreased free volume when compared to an even-membered spacer. This would be expected to increase the glass transition temperature of an odd member relative to an even-membered spacer. The less regular behaviour of the clearing temperatures seen for early

members of the series, for which only nematic behaviour is observed, would also be expected given that there are no particular steric considerations for the arrangement of the side chains in the nematic phase as there are in the smectic A phase. It is not clear, however, why the nematic-isotropic transition temperature for 2-MeOAzB is considerably higher than those of the other members of the series. Anomalously low nematic-isotropic transition temperatures have been observed for the propyl member of other polymethacrylate-based series and suggests that the spacer is too short to allow the mesogenic groups to maximise their interactions [48]. The corresponding homologous series to the n-MeOAzB series but based on a polystyrene backbone have been reported [51,60,61] and these only show the smectic A_1 phase. The transition temperatures of the two series are comparable as would be expected given that the flexibility of the two backbones is similar [45].

4. Conclusions

We have reported, for the first time, the liquid crystal properties of the homologous series, the poly[ω-(4-methoxyazobenzene-4'-oxy)alkyl methacrylate]s, members of which have been extensively studied for their photoresponsive behaviour. All nine homologues prepared as part of this study exhibited liquid crystal behaviour. For short spacer lengths, nematic behaviour was observed and on increasing spacer length, a smectic A_1 phase emerged. The driving force for the formation of the SmA_1 phase is believed to be the optimisation of the packing efficiency of the side-chains while the backbones are confined to lie between the smectic layers. The formation of a partially interdigitated smectic A phase in which the mesogenic groups overlapped would maximise the interactions between the liquid crystal groups but not fill spacer efficiently. Incommensurate smectic behaviour was observed for the nonyl member. Odd-even effects seen in the transition temperatures of these polymers on varying the length of the spacer may be understood in terms of the average shape of the side chain and its dependence on the parity of the spacer.

References

[1]   Shibaev, V.P. *Polym. Sci. Ser. A*, **2009**, *51*, 1131-1193

[2]   Ichimura, K. *Chem. Rev.*, **2000**, *100*, 1847-1874

[3]   Ikeda, T. *J. Mater. Chem.*, **2003**, *13*, 2037-2057

[4]   Eelkema, R. *Liq. Cryst.,* **2011**, *38*, 1641-1652

[5]   Prasad, S.K.; Nair, G.G.; Rao, D.S.S. *Liq. Cryst.*, **2009**, *36*, 705-716

[6] Tamba, M.G.; Bobrovsky, A.; Shibaev, V.; Pelzl, G.; Baumeister, U.; Weissflog, W. *Liq. Cryst.*, **2011**, *38*, 1531-1550

[7] Budagovsky, I.A.; Ochkin, V.N.; Smayev, M.P.; Zolot'ko, A.S.; Bobrovsky, A. Yu.; Boiko, N.I.; Lysachkov, A.I.; Shibaev, V.P.; Barnik, M.I. *Liq. Cryst.*, **2009**, *36*, 101-107

[8] González-Henríquez, C.M.; Soto-Bustamante, E.A.; Waceols-Gordillo, D.A.; Haase, W. *Liq. Cryst.*, **2009**, *36*, 541-547

[9] Alicante, R.; Cases, R.; Villacampa, B.; Oriol, L. *Macromol. Chem. Phys.*, **2010**, *211*, 2218-2225

[10] Shishido, A. *Polym. J.*, **2010**, *42*, 525-533

[11] Han, D.H.; Tong, X.; Zhao, Y.; Galstian, T.; Zhao, Y. *Macromolecules*, **2010**, *43*, 3664-3671

[12] González Henríquez, C.M.; Soto Bustamante, E.A.; Waceols Gordillo, D.A.; Haase, W. *Liq. Cryst.*, **2010**, *37*, 217-225

[13] Bobrovsky, A.; Shibaev, V.; Bubnov, A.; Hamplova, V.; Kaspar, M.; Pociecha, D.; Glogarova, M. *Macromol. Chem. Phys.*, **2011**, *212*, 342-352

[14] Yamada, M.; Kondo, M.; Mamiya, J.-I.; Yu, Y.; Kinoshita, M.; Barrett, C.J.; Ikeda, T. *Angew. Chem. Int. Ed.*, **2008**, *47*, 4986-4988

[15] Deng, W.; Li, M.-H.; Wang, X.; Keller, P. *Liq. Cryst.*, **2009**, *36*, 1023-1029

[16] Corbett, D.; Warner, M. *Liq. Cryst.*, **2009**, *36*, 1263-1280

[17] Kondo, M.; Miyasato, R.; Naka, Y.; Mamiya, J.-I.; Kinoshita, M.; Yu, Y.; Barrett, C.J.; Ikeda, T. *Liq. Cryst.*, **2009**, *36*, 1289-1293

[18] Lee, K.M.; Koerner, H.; Vaia, R.A.; Bunning, T.J.; White, T.J. *Macromolecules*, **2010**, *43*, 8185-8190

[19] Garcia-Amoros, J.; Finkelmann, H.; Velasco, D. *J. Mater. Chem.*, **2011**, *21*, 1094-1101

[20] He, C.; Zhang, C.; Zhang, O. *Liq. Cryst.*, **2009**, *36*, 379-387

[21] Wang, Q.; Yang, C.; Xie, H.; Wang, X.; Zhang, H. *Liq. Cryst.*, **2010**, *37*, 435-443

[22] Yang, C.-A.; Wang, Q.; Xie, H.; Zhong, G.; Zhang, H. *Liq. Cryst.*, **2010**, *37*, 1339-1346

[23] Muzzalupo, R.; Ranieri, G.A.; Catalando, D.; Galli, G.; Veracini, C.A. *Liq. Cryst.*, **1995**, *19*, 367-371

[24] Walther, M.; Faulhammer, H.; Finkelmann, H. *Macromol. Chem. Phys.*, **1998**, *199*, 223-237

[25] Zhang, H.C.; He, W.D.; Pan, C.Y. *Acta Polym. Sinica.*, **1999**, 100-106

[26] Cook, A.G.; Imrie, C.T. *Mol. Cryst. Liq. Cryst.*, **1999**, *332*, 2699-2708

[27] Han, M.; Morino, S.; Ichimura, K. *Macromolecules*, **2000**, *33*, 6360-6371

[28] Han, M.; Ichimura, K. *Macromolecules*, **2001**, *34*, 82-89

[29] Han, M.; Ichimura, K. *Macromolecules*, **2001**, *34*, 90-98

[30] Hore, D.K.; Natansohn, A.L.; Rochon, P.L. *J. Phys. Chem. B*, **2003**, *107*, 2506-2518

[31] Kawatsuki, N.; Uchida, E.; Yamamoto, T. *Macromol. Chem. Phys.*, **2003**, *204*, 584-590

[32] Cui, L.; Zhao, Y.; Yavrian, A.; Galstian, T. *Macromolecules*, **2003**, *36*, 8246-8252

[33] Uchida, E.; Shiraku, T.; Ono, H.; Kawatsuki, N. *Macromolecules*, **2004**, *37*, 5282-5291

[34] Kawatsuki, N.; Uchida, E.; Ono, H. *Chem. Lett.*, **2004**, *33*, 12-13

[35] Kawatsuki, N.; Shiraku, T.; Uchida, E. *Mol. Cryst. Liq. Cryst.*, **2005**, *441*, 163-171

[36] Uchida, E.; Kawatsuki, N. *Polymer*, **2006**, *47*, 2322-2329

[37] Uchida, E.; Kawatsuki, N. *Polym. J.*, **2006**, *38*, 724-731

[38] Tejedor, R.M.; Oriol, L.; Serrano, J.L.; Ureña, F.P.; González, J.L.L. *Adv. Funct. Mater.*, **2007**, *17*, 3486-3492

[39] He, X.; Sun, W.; Yan, D.; Xie, M.; Zhang, Y. *J. Polym. Sci.: Part A: Polym. Chem.*, **2008**, *46*, 4442-4450

[40] Zhu, X.-Q.; Liu, J.-H.; Liu, Y.-X.; Chen, E.-Q. *Polymer*, **2008**, *49*, 3103-3110

[41] Stewart, D.; Imrie, C.T. *Polymer*, **1996**, *37*, 3419-3425

[42] Henderson, P.A.; Cook, A.G.; Imrie, C.T. *Liq. Cryst.*, **2004**, *31*, 1427-1434

[43] Craig, A.A.; Imrie, C.T. *J. Mater. Chem.* **1994**, *4*, 1705-1714

[44] Imrie, C.T.; Karasz, F.E.; Attard, G.S. *J. Macromol. Sci. – Pure Appl. Chem.*, **1994**, *A31*, 1221-1232

[45] Craig, A.A.; Imrie, C.T. *Macromolecules*, **1999**, *32*, 6215-6220

[46] Imrie, C.T.; Karasz, F.E.; Attard, G.S. *Macromolecules*, **1993**, *26*, 3803-3810

[47] Imrie, C.T.; Taylor, L. *Liq. Cryst.*, **1989**, *6*, 1-10

[48] Craig, A.A.; Winchester, I.; Madden, P.C.; Larcey, P.; Hamley, I.W.; Imrie, C.T. *Polymer*, **1998**, *39*, 1197-1205

[49] McMillan, W.L. *Phys. Rev. A*, **1971**, *4*, 1238-1246

[50] Date, R.W.; Imrie, C.T.; Luckhurst, G.R.; Seddon, J.M. *Liq. Cryst.*, **1992**, *12*, 203-238

[51] Schleeh, T.; Imrie, C.T.; Rice, D.M.; Karasz, F.E.; Attard, G.S. *J. Polym. Sci.: Part A: Polym. Chem.*, **1993**, *31*, 1859-1869

[52] Craig, A.A.; Imrie, C.T. *Polymer*, **1997**, *38*, 4951-4957

[53]   Imrie, C.T. *Liq. Cryst.*, **2006**, *33*, 1449-1454

[54]   Yeap, G.Y.; Hng, T.C.; Yeap, S.Y.; Gorecka, E.; Ito, M.M.; Ueno, K.; Okamoto, M.; Mahmood, W.A.K.; Imrie, C.T. *Liq. Cryst.*, **2009**, *36*, 1431-1441

[55]   Donaldson, T.; Henderson, P.A.; Achard, M.F.; Imrie, C.T. *Liq. Cryst.*, **2011**, *38*, 1331-1339

[56]   Imrie, C.T.; Schleeh, T.; Karasz, F.E.; Attard, G.S. *Macromolecules*, **1993**, *26*, 539-544

[57]   Craig, A.A.; Imrie, C.T. *Macromolecules*, **1995**, *28*, 3617-3624

[58]   Attard, G.S.; Dave, J.S.; Wallington, A.; Imrie, C.T.; Karasz, F.E. *Makromol. Chem.,* **1991**, *192*, 1495-1508

[59]   Hamley, I.W.; Fairclough, J.P.A.; King, S.M.; Pedersen, J.S.; Richardson, R.M.; Imrie, C.T.; Craig, A.A. *Liq. Cryst.*, **1997**, *22*, 679-684

[60]   Imrie, C.T.; Karasz, F.E.; Attard, G.S. *Liq. Cryst.*, **1991**, *9*, 47-57

[61]   Imrie, C.T.; Karasz, F.E.; Attard, G.S. *Macromolecules*, **1992**, *25*, 1278-1283

Figure captions

Scheme Synthetic route used to prepare the *n*-MeOAzB series, **1**.

Figure 1 Normalised DSC traces obtained on the second heating of the *n*-MeOAzB series, **1**.

Figure 2 (a) Nematic *schlieren* texture (132 ˚C) and (b) smectic A focal conic fan texture (120 ˚C) exhibited by 10-MeOAzB.

Figure 3 (a) The small and (b) the wide angle X-ray diffraction patterns obtained for 3-MeOAzB at 100 ˚C. The sharp peaks observed at $2\theta = 38˚$ and $44˚$ in (b) arise from the mica sheet used to contain the sample.

Figure 4 Deconvolution of the clearing endotherm in the DSC reheating trace of 10-MeOAzB revealing the SmA-N and N-I transitions.

Figure 5 (a) The small and (b) the wide angle X-ray diffraction patterns obtained for 10-MeOAzB at 110 ˚C.

Figure 6 (a) The small and (b) the wide angle X-ray diffraction patterns obtained for 9-MeOAzB at 115 ˚C.

Figure 7 (a) The small and (b) the wide angle X-ray diffraction patterns obtained for 9-MeOAzB at 135 ˚C.

Figure 8 The temperature dependence of the small angle X-ray diffraction as a function of the scattering vector, q for 9-MeOAzB. The peaks are $q = 0.241$ Å^{-1}, $d = 26.1$ Å and $q = 0.443$ Å^{-1}, $d = 14.2$ Å.

Figure 9 Possible packing of the side-chains in the smectic A phase of 9-MeOAzB: (a) the smectic A_1 phase in which the side chains are fully interleaved and (b) an incommensurate phase in which domains of parallel aligned side chains (shown in red) coexist with the SmA1 phase.

Figure 10 The dependence of the transition temperatures on the number of methylene units, *n*, in the flexible alkyl spacer for the *n*-MeOAzB series. ○ denotes the glass transition, ☐ the nematic-isotropic transition, ☐ the smectic A-isotropic transition and ☐ the smectic A-nematic transition. The data for 2-MeOAzB [33] and12-MeOAzB [40] have been taken from the literature.

Figure 11 Sketches of the shape of the side chain containing (a) an even and (b) an odd number of methylene units in the flexible spacer.

Table 1.   Molecular weights, polydispersities (*PD*) and number average degrees of polymerisation (*DP*) for the *n*-MeOAzB series, **1**.

n	$_w$ / g mol^{-1}	$_n$ / g mol^{-1}	*PD*	P
3	53300	23800	2.2	67
4	29000	10400	2.8	28
5	28800	10300	2.8	27
6	58100	22800	2.6	58
7	60300	32300	1.9	79
8	22800	10000	2.3	23
9	63700	23750	2.7	54
10	44500	18000	2.5	40
11	20800	7000	3.0	15

Table 2. Thermal properties of the *n*-MeOAzB series, **1**, extracted from the reheating DSC trace.

n	T_g / °C	T_{SmAN} / °C	$\Delta S_{SmAN}/R$	T_{NI} / °C T_{SmAI} / °C†	$\Delta S_{NI}/R$ $\Delta S_{SmAI}/R$†
3	78			122	0.23
4	80			140	0.42
5	88	110	0.56	135	0.44
6	78	95	0.38	135	0.47
7	89			140†	2.14†
8	76	119	0.55	136	0.50
9	81			146†	2.37†
10	77			137[a]	1.85 [a]
11	74			145†	2.56†

[a] Combined SmA-N-I transition. Deconvolution of the peak into two gives: T_{SmAN} = 127 °C, $\Delta S_{SmAN}/R$ = 0.73, T_{NI} = 134 °C and $\Delta S_{NI}/R$ = 1.48 (see text and Figure 4).

Figure 1
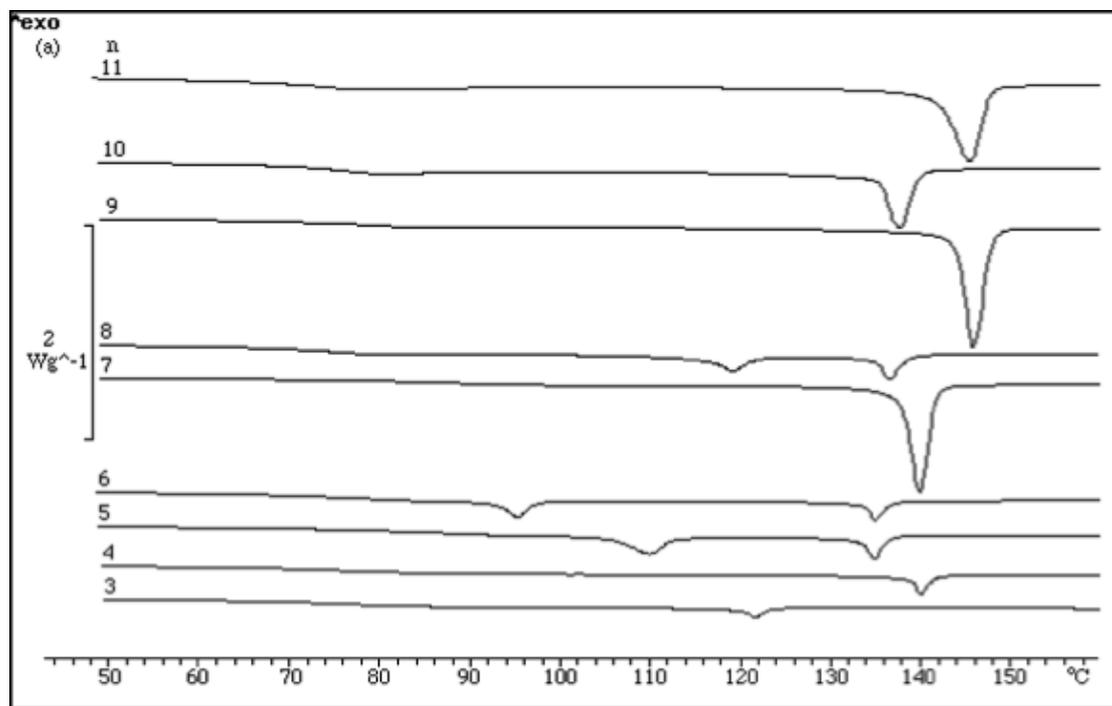
Figure 2(a)
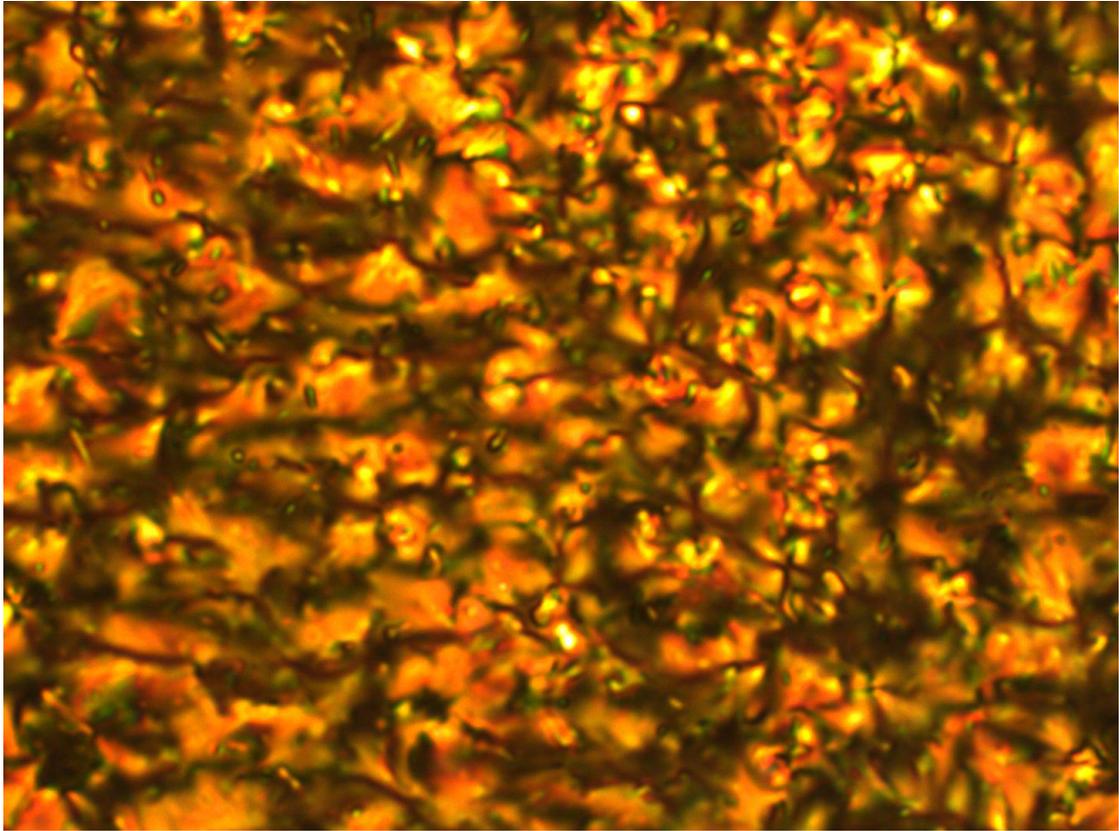
Figure 2(b)

Figure 3

(a)

(b)

Figure 4

ΔH_{NI} = 5.00 KJ/mol
T_p = 134 ºC

ΔH_{SmAN} = 2.41 KJ/mol
T_p = 127 ºC

endo

h$_f$ (W/g)

T (ºC)

90   100   110   120   130   140   150
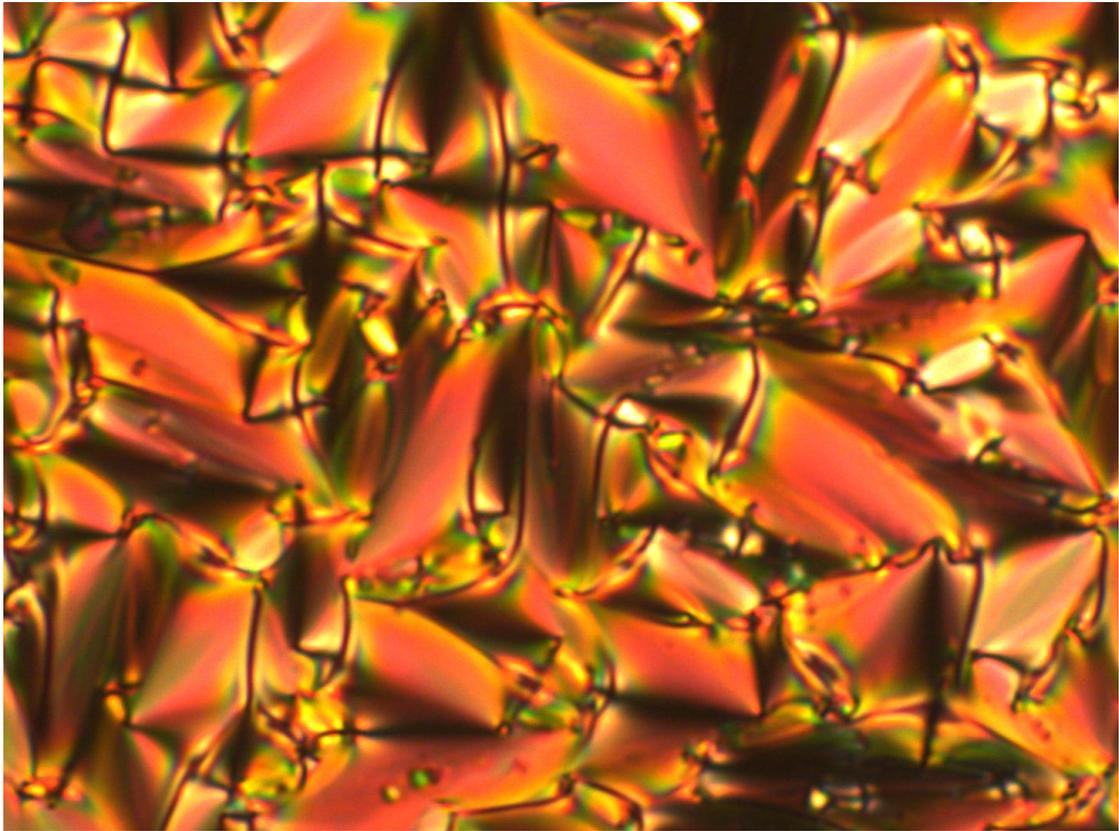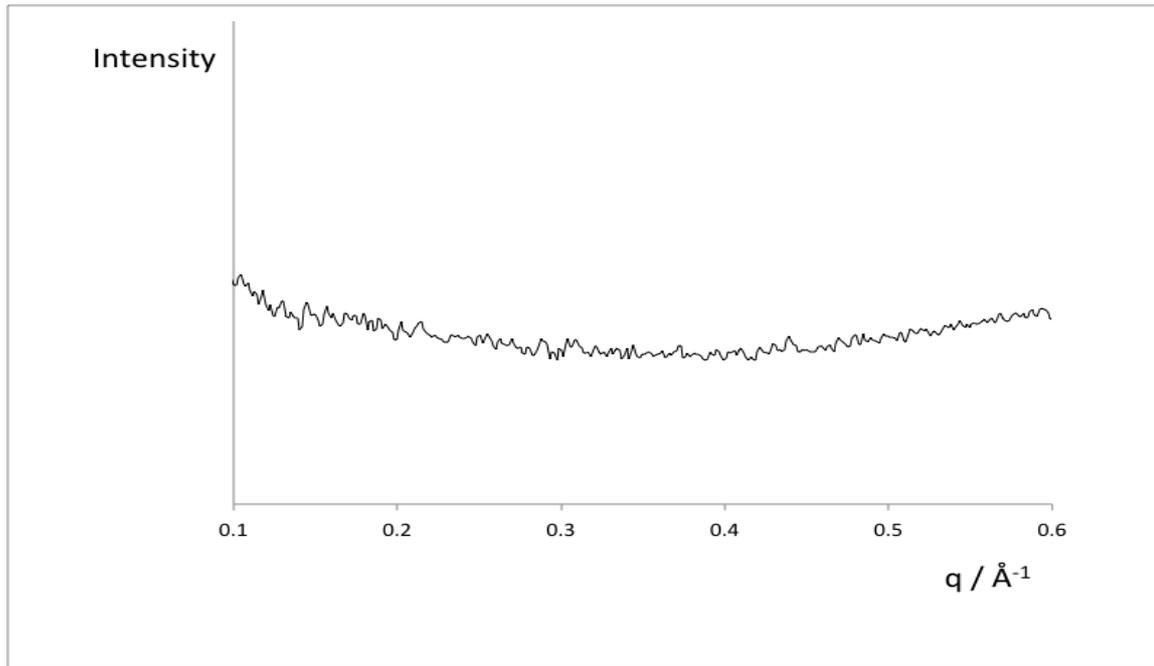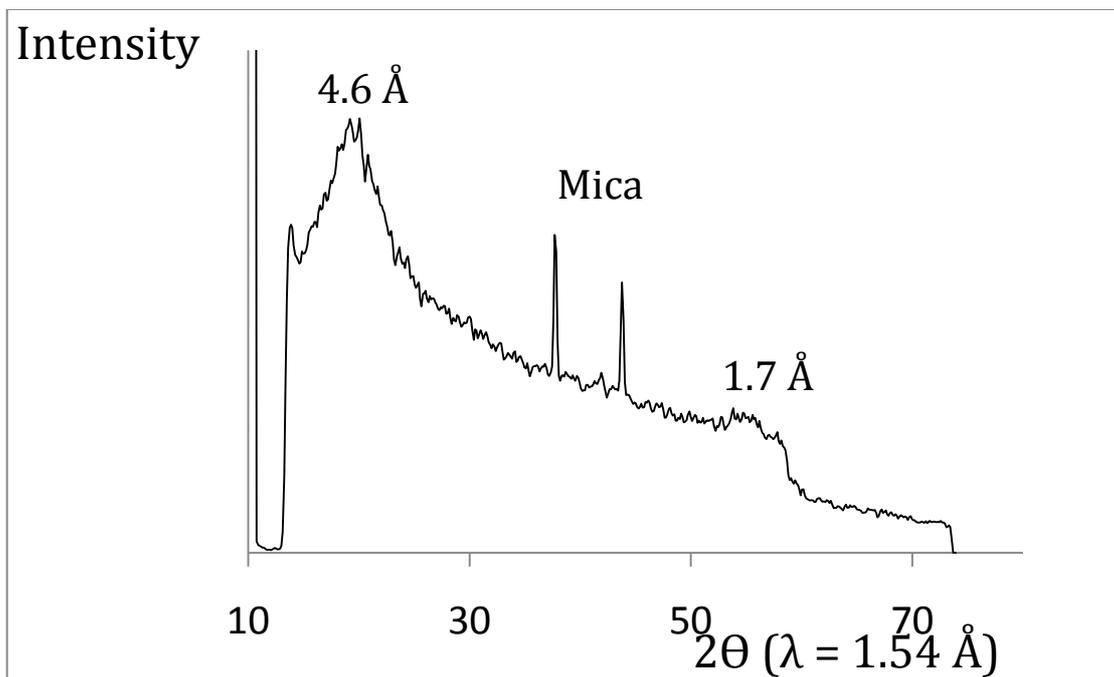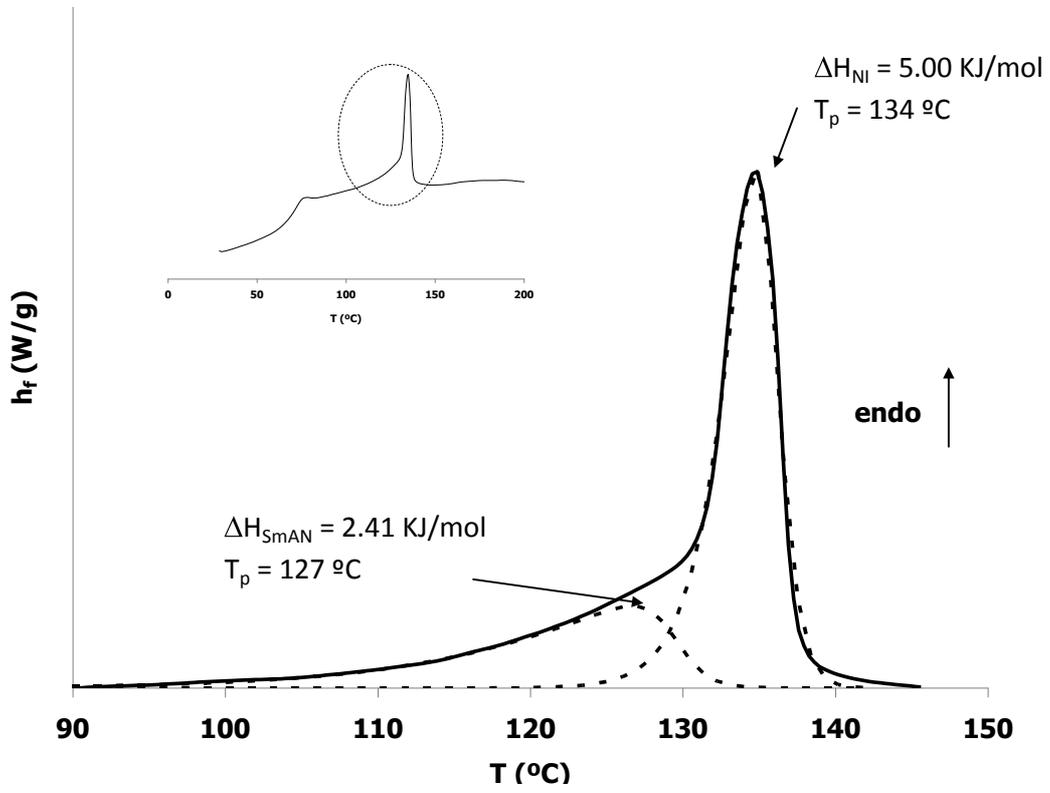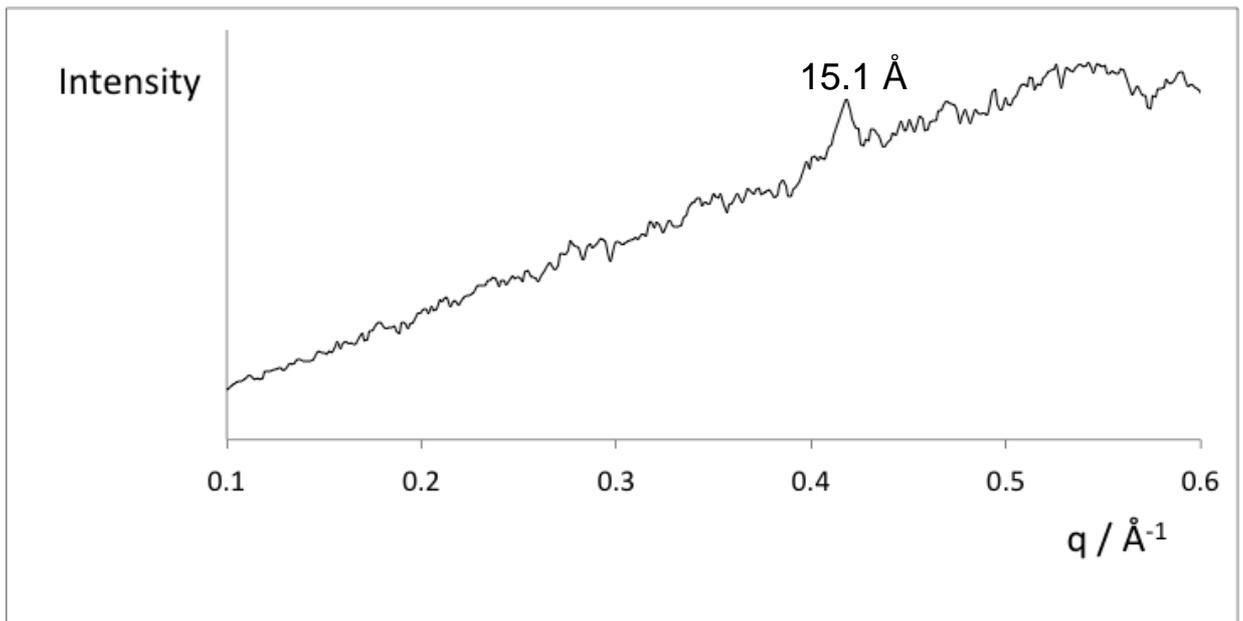
(a)
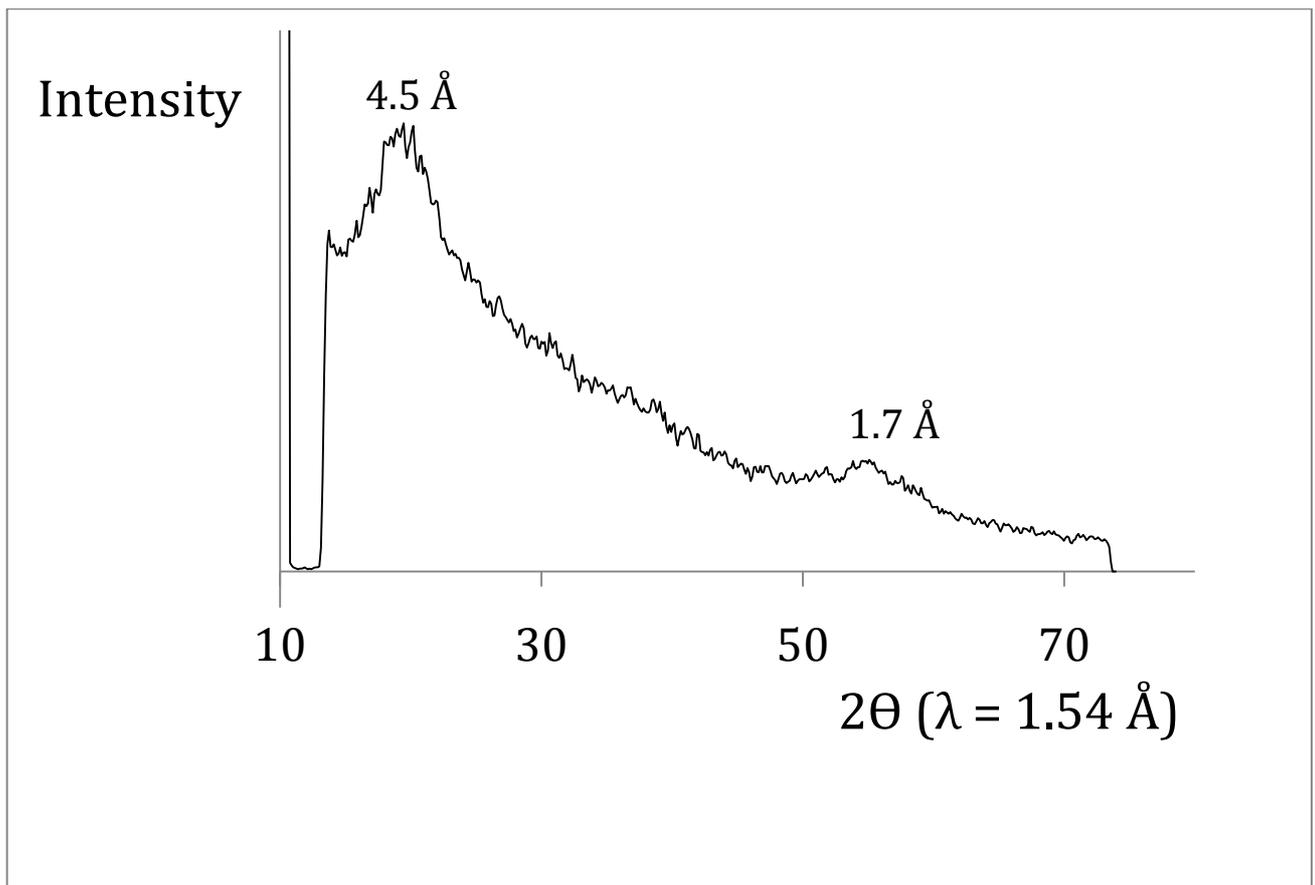
(b)
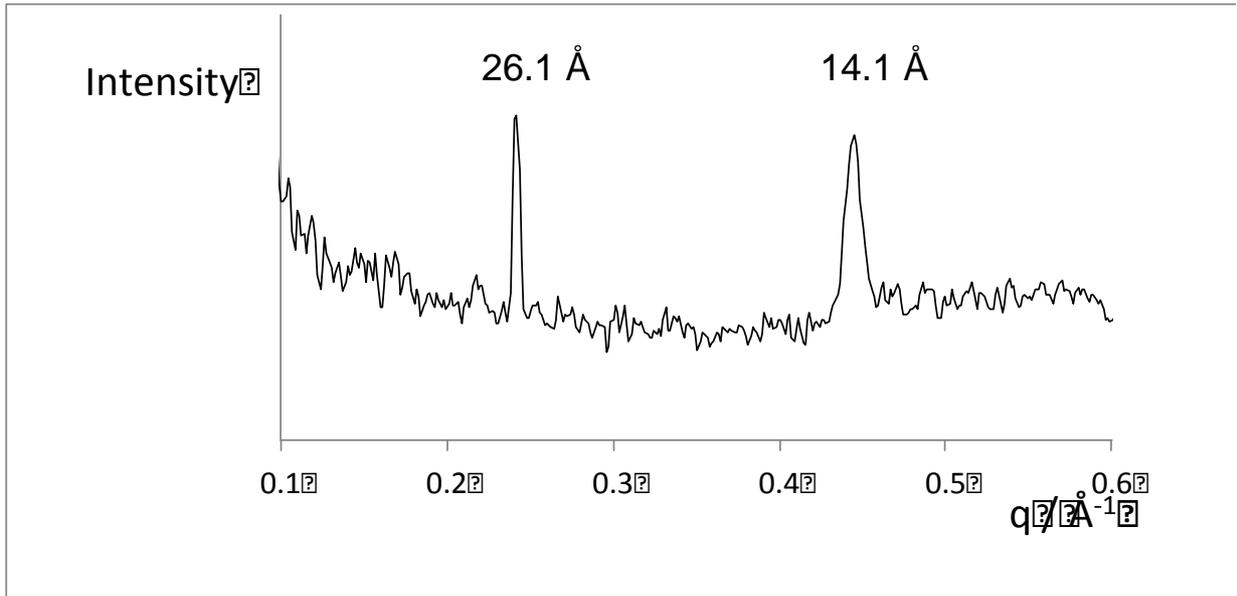
Figure 5

(a)
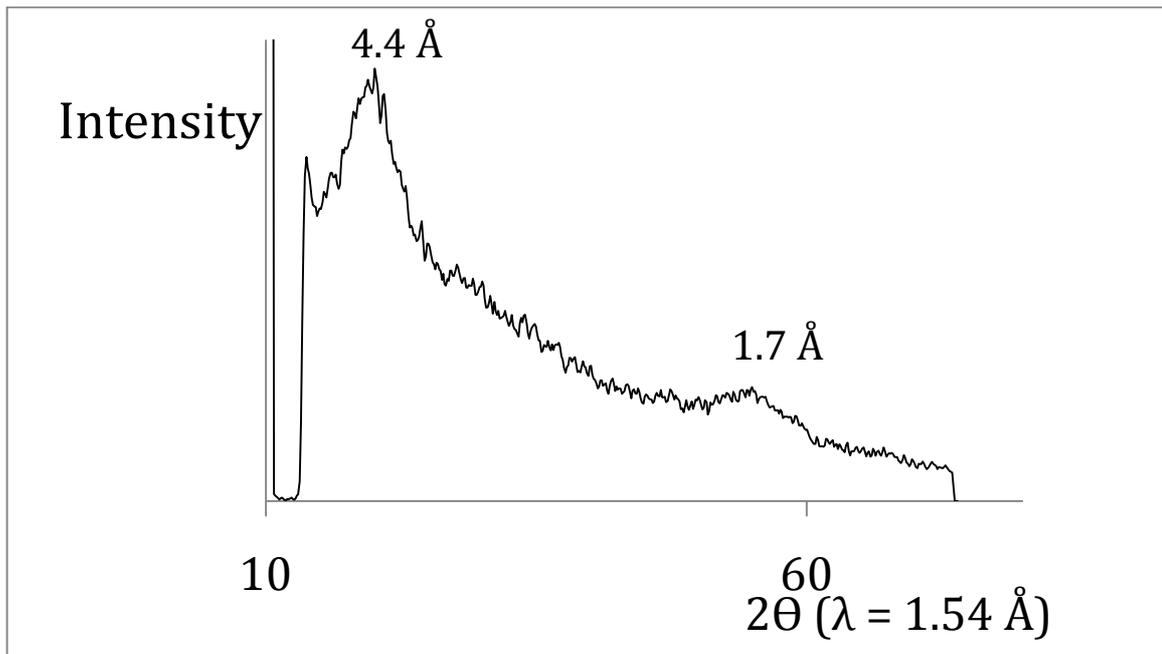
(b)
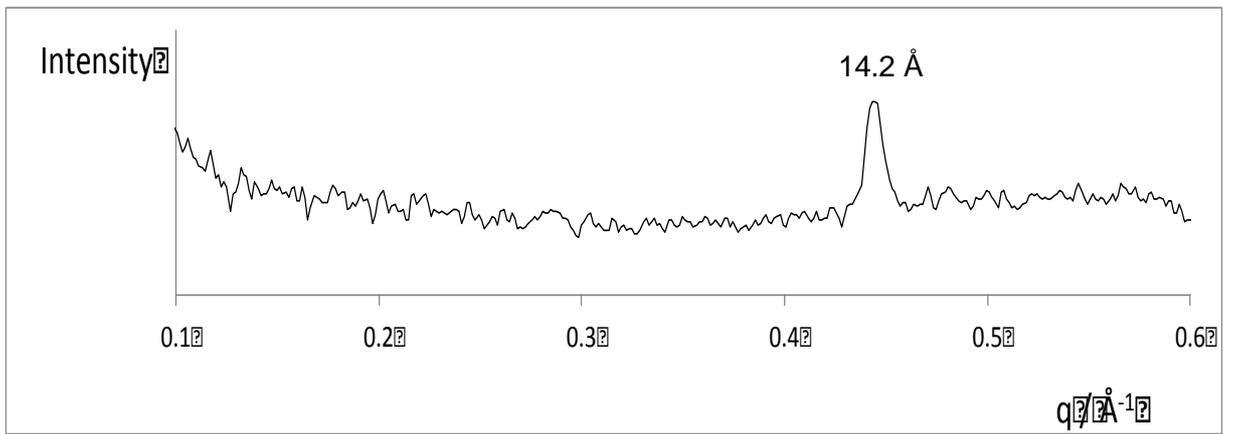
Figure 6

(a)
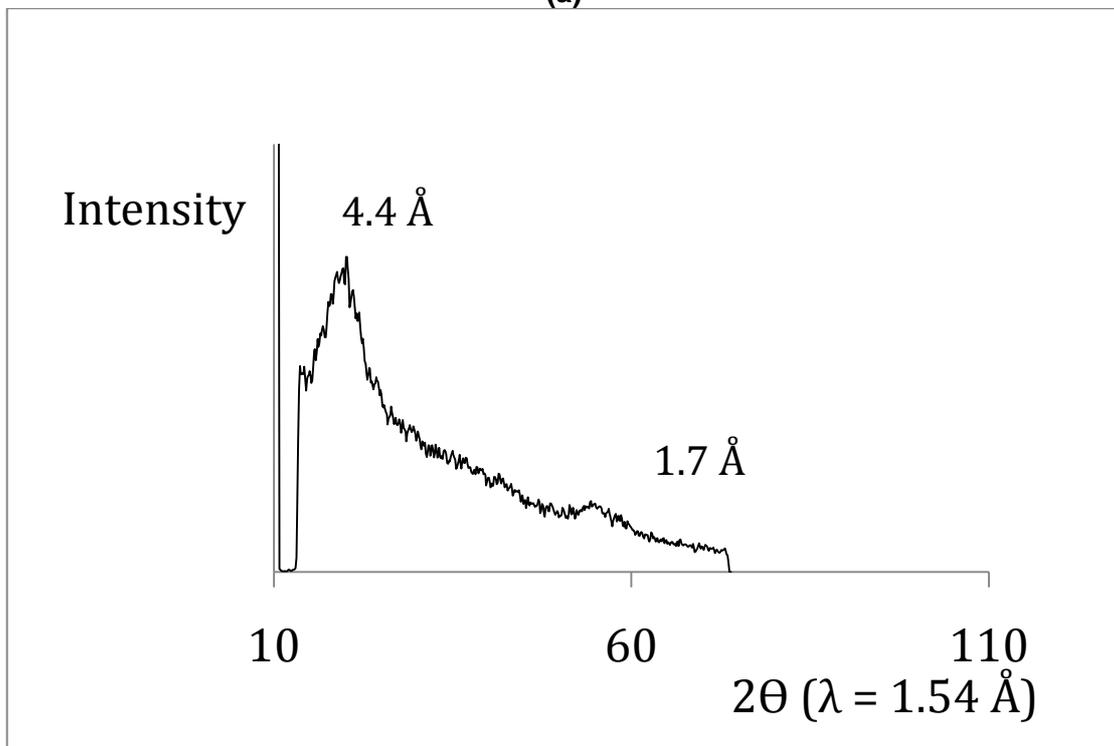
(b)

Figure 7

Figure 8

Figure 9

Figure 10

(a)

(b)

Figure 11

Scheme 1